International Journal of Automation and Computing

16(5), October 2019, 671-682
DOI: 10.1007/s11633-018-1153-8

A Robust Face Recognition Method Combining LBP with Multi-mirror Symmetry for Images with Various Face Interferences

Shui-Guang Tong[1,2] Yuan-Yuan Huang[1,2] Zhe-Ming Tong[1,2]

[1]State Key Laboratory of Fluid Power and Mechatronic Systems, Zhejiang University, No.38, Zheda Road, Hangzhou 310027, China

[2]School of Mechanical Engineering, Zhejiang University, No.38, Zheda Road, Hangzhou 310027, China

Abstract: Face recognition (FR) is a practical application of pattern recognition (PR) and remains a compelling topic in the study of computer vision. However, in real-world FR systems, interferences in images, including illumination condition, occlusion, facial expression and pose variation, make the recognition task challenging. This study explored the impact of those interferences on FR performance and attempted to alleviate it by taking face symmetry into account. A novel and robust FR method was proposed by combining multi-mirror symmetry with local binary pattern (LBP), namely multi-mirror local binary pattern (MMLBP). To enhance FR performance with various interferences, the MMLBP can 1) adaptively compensate lighting under heterogeneous lighting conditions, and 2) generate extracted image features that are much closer to those under well-controlled conditions (i.e., frontal facial images without expression). Therefore, in contrast with the later variations of LBP, the symmetrical singular value decomposition representation (SSVDR) algorithm utilizing the facial symmetry and a state-of-art non-LBP method, the MMLBP method is shown to successfully handle various image interferences that are common in FR applications without preprocessing operation and a large number of training images. The proposed method was validated with four public data sets. According to our analysis, the MMLBP method was demonstrated to achieve robust performance regardless of image interferences.

Keywords: Face recognition (FR), local binary pattern (LBP), facial symmetry, image interferences, multi-mirror average.

1 Introduction

Pattern recognition (PR) has attracted great attention worldwide over recent decades, and its application in the field of face recognition (FR) also remains a hot topic due to its vital position in systems used for automatic face analysis. As a result, a variety of FR methods have been proposed with promising results[1–6]. Most of the research work has focused on FR under relatively well-controlled conditions, that is to say, the recognition task is carried out with frontal expressionless images under uniform illumination. However, for practical applications, the performance of FR is generally influenced by objective factors. Varying face ages[7–9], image resolution[10–12], facial expressions[13–15], body poses[16–18] and illumination conditions[19–21] all cause changes to face representations, resulting in a rapid decline in FR performance. This paper focuses on the illumination, occlusion, facial expression and pose interference, which are common and major challenges in real-world applications of FR. Researchers have shown that the performance of the FR algorithm can be severely affected by those interferences[14]. Therefore, a large number of research studies have focused on these problems in order to obtain a better representation of the original face image.

Changes in illumination conditions can degrade FR performance. Methods to tackle this problem can be classified into three categories: preprocessing methods, subspace learning-based approaches and illumination-invariant feature extraction methods. Preprocessing methods such as histogram equalization (HE)[22, 23], logarithm transform (LT)[24], and gamma correction (GC)[25] attempt to take the holistic normalization of the original face images so that the obtained representations are consistent with those under uniform illumination conditions. Since the same face images under varying illumination conditions can be approximated by a low dimensional linear subspace[26, 27], the original face images with high-dimensional data are modeled by a small subset of features for classification and recognition. A series of subspace learning-based approaches like principal component analysis (PCA), independent component analysis (ICA), and linear discriminant analysis (LDA) and some improved algorithms have been put forward. In general, these methods can be seen as a means of dimensionality reduc-

Research Article
Manuscript received April 18, 2018; accepted August 7, 2018; published online November 19, 2018
Recommended by Associate Editor De Xu

tion and they can model the illumination variation quite well. Illumination-invariant feature extraction methods, such as Retinex, quotient image (QI)[28, 29] and gradient face (GF)[30], on the other hand, make use of local features to rebuild the illumination-invariant face representations.

The illumination problems discussed above can be divided into two categories: varying lighting magnitude and varying lighting directions. Varying lighting magnitude can also be called homogeneous lighting which assumes that the directions of the light are the same, and this is the basic hypothesis in most of the existing research. However, in practical applications, the lighting conditions are not always homogeneous. The recognition task is normally carried out under the condition of varying lighting directions, namely heterogeneous lighting. Therefore, there is a lot of work to be done to resolve the heterogeneous lighting problem.

Facial occlusion is considered one of the greatest challenges affecting the accuracy of the FR system. Common occlusions include hats, scarves, sunglasses, and exaggerated facial expressions. These occlusions may undermine the original face image, causing loss of significant information and thus leading to misclassification. Much research has been done to handle the occlusion problem and can be roughly classified into two categories: traditional holistic feature-based approaches[2] and local feature-based approaches[31, 32]. Holistic feature-based approaches consider the holistic normalization of the whole face image, while local feature-based approaches concentrate on only the occluded face part and match it with the non-occluded training images. The local feature-based approaches are more robust to facial occlusions.

FR across various pose conditions allows us to recognize the same person with varying poses in both training and testing sets. A more challenging task is to recognize a person in varying poses with only one frontal image available in the training set. This problem is one of the unsolved puzzles in the FR system, but some promising methods have been put forward to tackle the problem and can be classified into 2D techniques[33, 34] and 3D techniques[35, 36]. The 3D techniques gather 3D information to establish a virtual face image that is the same as the image given at a given pose. Thus, two face images from two different poses can match each other at the same pose. The 2D techniques, on the other hand, attempt to identify pose-invariant local features to overcome pose variation problems.

Compared to FR using illumination and pose variation, the study of the interference of facial expression has been less investigated. Facial expressions can be seen as muscle deformation, which is commonly used to convey our emotions. However, in a practical FR system, changes in expression can degrade recognition performance and the bigger the deformation, the worse the recognition performance. Various approaches have been put forward to overcome facial expression variation problems[15]. These methods have one thing in common, i.e., they all extract local features to recognize frontal faces varying in expression, since local features are more robust to expression changes than holistic ones.

The local binary pattern (LBP) method, introduced by Ojala et al.[37], was first used as a powerful texture descriptor. In 2004, Ahonen et al.[38, 39] applied LBP to the field of FR and achieved great success. Since then, a great deal of research has been done to apply the LBP algorithms for executing FR tasks. However, the original LBP operator can only achieve perfect results under well-controlled conditions. When there are interferences such as heterogeneous illumination, occlusion, facial expression and pose variation, the obtained LBP performance will be affected. Many researchers have been devoted to tackling this problem. Methods like improved LBP (ILBP)[40], multiscale block LBP (MBLBP)[41] and local ternary pattern (LTP)[21] can solve the problem to a degree, but not completely. In this study, we proposed a novel interference-robust approach to FR based on LBP and facial symmetry, called multi-mirror local binary patterns (MMLBP). Compared with the original LBP, the method utilizing the facial symmetry based on original image (SORI), its later variations (ILBP, MBLBP and LTP), the symmetrical singular value decomposition (SSVDR) algorithm utilizing the facial symmetry[42] and a state-of-art non-LBP method multi-directional multi-level dual-cross patterns (MDML-DCPs)[43], the proposed method is more robust to FR with interferences and can achieve better recognition performance. Furthermore, the method is also suitable for FR systems with only few training images or even one frontal expressionless face image under uniform illumination available in the training set, which is a big challenge in FR[44].

The results of LBP codes can be collected into a histogram or represented with an LBP feature image. According to the research provided by Yang and Chen[45], the LBP feature image is more suitable for FR with large interferences. As a result, the strategy of this paper is to calculate the LBP codes for each pixel and represent it as an LBP feature image as a whole. The reasons are given as follows:

1) The local LBP features by its definition shows great robustness and high discriminative power.

2) The LBP feature image faithfully preserves both spatial structure and intrinsic appearance details of a face image. Specifically, the obtained feature is also a face image.

3) The LBP feature image dispenses with the preprocessing of region division and the post-processing of histogram, and thus it is computationally efficient.

4) The LBP feature image is more effective for FR, but it is not suitable for texture recognition. The reason is that the texture images have specific statistic properties.

The rest of this paper is organized as follows: Section 2 details the related work. Section 3 presents the proposed method. The results of the experiments are described in Section 4. Section 5 provides the concluding remarks.

2 Related work

Local binary patterns were introduced by Ojala in 1996 as a powerful texture descriptor. It is defined in a 3×3 neighborhood, and the gray value of the adjacent 8 pixels is compared with the pixel at the center of the window as a threshold, if the value is larger than that of the center point, then it is denoted as 1, otherwise it is 0, as represented in (1).

$$s(x) = f(x) = \begin{cases} 1, & x > 0 \\ 0, & x \le 0. \end{cases} \tag{1}$$

Thus, we can get an 8-bit binary number, and then sum them up with a weight of 2^p, obtaining an LBP value.

$$LBP(x_c, y_c) = \sum_{p=0}^{p=7} s(g_p - g_c)\, 2^p \tag{2}$$

where g_c represents the gray value of the center point of the local region, $g_p(p=0, 1, \cdots, 7)$ corresponds to the 8 points of neighborhood distribution around the center point. The illustration of the basic LBP operator can be seen in Fig. 1(a).

One major drawback of the basic LBP operator is that it covers only a small area, which obviously cannot meet the needs of different sizes of textures. Later the operator was extended to a neighborhood of different sizes, more specifically, the 3×3 square neighborhood is replaced by a circular one with P pixels in the neighborhood of radius R, named LBP_P^R. Another extension of the basic LBP operator is called "uniform patterns", which aims to solve the information explosion problem. An LBP can be called uniform if the binary pattern contains up to two transitions from 0 to 1 or 1 to 0. For instance, the LBP code in Fig. 1(a) is not uniform since there are four transitions. To get the rotation invariant LBP operator, the idea is to constantly rotate the circular neighborhood to get a series of initial LBP values, where the minimum one can be recognized as the final LBP value. Fig. 1(b) shows the process of finding the rotation invariant LBP operator. By combining the three extensions above, we obtain a rotation invariant uniform pattern, which reduces the possible pattern types from 2^p to $p+1$, and all non-uniform patterns are classified as $p+1$, as shown in (3).

$$LBP_{P,R}^{riu2} = \begin{cases} \sum_{p=1}^{p-1} s(g_p - g_c), & U(G_P) \le 2 \\ P+1, & U(G_P) > 2 \end{cases} \tag{3}$$

where $U(G_P)$ represents the bitwise transitions from 0 to 1 or from 1 to 0, LBP^{riu2} is called the rotation invariant uniform pattern.

The LBP operator was first applied to FR by Ahonen et al.[38] in 2004. The specific methodology of this application can be broken into three steps: First the given face image is divided into small local regions, then the LBP algorithm is performed on each local region to obtain its LBP feature. Finally concatenate all the local LBP features to form the global feature of the whole face which can be used to carry out the FR tasks.

3 Methodology with MMLBP

3.1 LBP used for FR under varying interferences

Illumination, occlusion, facial expression and pose interferences have always been major challenges in practical FR systems. It often leads to some undesirable problems. Therefore, to verify the interference robustness of the LBP operator used for FR, we compared its performance under varying interference conditions, which can be classified into four groups as mentioned above: illumination, occlusion, facial expression and pose. In the experiment, the face images are chosen from the Yale B, AR, and facial recognition technology (FERET) databases. The visual represents are shown in Fig. 2.

In Fig. 2, the basic LBP operator can establish a good representation of the original face images under a well-

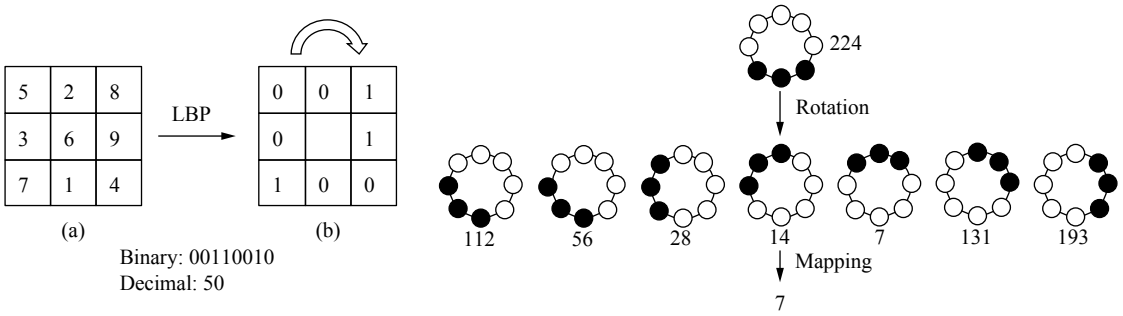

Fig. 1 Basic LBP operator and an improved version of it. (a) Basic LBP operator; (b) Rotation invariant LBP.

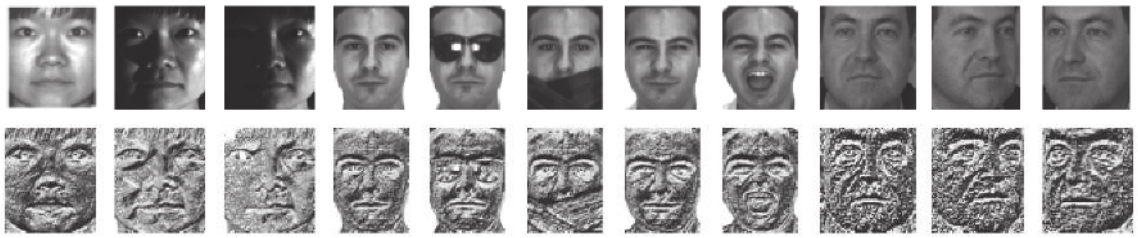

Fig. 2 LBP used for FR under varying interference

controlled condition (the first image of each person). However, when there are various interferences, the representations are not intact and perfect. If the following FR task is carried out with only one frontal expressionless face image under uniform illumination available in the training set, recognition performance will be affected. To solve this problem, we made further efforts to find the cause of this phenomenon.

One of the common characteristics of human faces is that they are approximately bilaterally symmetrical. Based on this principle, Passalis et al.[17] used facial symmetry to handle pose variations in real-world 3D FR. Similarly, Chen et al.[42] put forward a symmetrical singular value decomposition (SSVDR) algorithm utilizing the facial symmetry for pattern recognition. Unlike these previous methods which simply mirror the half face, we combine the famous local binary pattern (LBP) with facial symmetry prior by dividing the face into multi-mirror regions and averaging the LBP representation of each region with the vertical flip matrix of its symmetric one without any preprocessing operation needed, which alleviate the interference and achieves higher recognition rate.

Although the proposed method utilizes facial symmetry, it is not always true that the human faces are perfectly symmetrical[17]. The method is based on the hypothesis that the difference between the right and left side of the same face image is less than that of two different face images. And the facial symmetry of the two sides of a face image can be measured by the index structure similarity ($SSIM$)[46]:

$$SSIM\,(x,y) = [l\,(x,y)]^{\alpha} \times [c\,(x,y)]^{\beta} \times [s\,(x,y)]^{\gamma} \qquad (4)$$

where x represents the left side of a face image, and y denotes the flip horizontal right side of a face image. $l\,(\cdot)$, $c\,(\cdot)$, and $s\,(\cdot)$ are the luminance comparison function, the contrast comparison function and the structure comparison function, respectively.

Here, we calculated the mean $SSIM$ of each LBP face image shown in Fig. 2, the results are presented in Table 1.

Seen from Table 1, the face images under well-controlled conditions have considerably higher $SSIM$ values. Those under varying interferences, however, have relatively low SSIM values. Therefore, we can conclude that image interferences like heterogeneous illumination, occlusion, facial expression and pose variation may lead to asymmetry of pixel values of the face image matrix, undermining the representations of the original face images. Hence, a natural idea to remove this obstacle is to reduce the asymmetry of pixel values of the face image when there are image interferences. According to this discovery, we extended the LBP operator and proposed a novel MMLBP method based on the symmetry of human face, which can greatly alleviate the influence of the image interferences.

3.2 Multi-mirror local binary patterns

As described above, we eliminated the effects of asymmetry caused by the interferences through the fact that humans are born with approximately symmetrical faces. We proposed a method called multi-mirror local binary patterns and before introducing our method, we first gave the definition of a vertical flip matrix as follows:

Definition (Vertical flip matrix). Suppose matrix $A{=}(a_{ij})_{m*n}$, if

$$B = \begin{bmatrix} a_{1n} & \cdots & a_{11} \\ \vdots & \ddots & \vdots \\ a_{mn} & \cdots & a_{m1} \end{bmatrix}$$

then the matrix B is called the vertical flip matrix of A, denoted as $B = A^{p}$.

According to the definition of vertical flip matrix, we can introduce one of its properties. If I_n represents the n-order unit matrix and its vertical flip matrix is J_n, which is also called the sub-unit matrix, then the vertical flip matrix of A can be rewritten as

$$A^{p} = AJ_n. \qquad (5)$$

The MMLBP method is broken down into the follow-

Table 1 Mean SSIM of each face images in Fig. 2

The image number	1	2	3	4	5	6	7	8	9	10	11
Mean SSIM values	**0.906**	0.092	0.126	**0.735**	0.496	0.419	0.561	0.653	**0.681**	0.217	0.317

ing steps:

First the given face image $A_{m\times n}$ is divided into multi-mirror regions along the direction parallel to the symmetric axis of the face. We use M to represent the number of mirrors, so we have $2M$ regions in total. To better describe our method, each region in the left half face is denoted as A_{Lk} (k=1, 2, ⋯, M), where k represents the position of each region in half face image and it increases from the face center to its border. Similarly, the regions in the right half face is denoted as A_{Rk} (k=1, 2,⋯ , M).

After obtaining these pre-defined regions, LBP is performed on each of them to extract local facial features. Here, the rotation invariant uniform LBP is employed, namely $LBP_{8,\ 1}{}^{riu2}$ (P=8, R=1). Detailed calculation is shown in the following formulas (here, we only give the calculation of the left half face, the right half face is the same):

$$LBP_{8,1}^{riu2}\left(A_{Lk}\left(i,j\right)\right)=\begin{cases}\sum_{p=0}^{7}s\left(g_p-g\left(i,j\right)\right)\times 2^p, & U\left(G_p\right)\le 2\\ 9, & U\left(G_p\right)>2,\quad k=1,2,\cdots,M\end{cases}\tag{6}$$

$$U\left(G_p\right)=\left|s\left(g_7-g(i,j)-s\left(g_0-g\left(i,j\right)\right)\right|+\sum_{p=1}^{7}\left|s\left(g_7-g\left(i,j\right)\right)-s\left(g_7-g\left(i,j\right)\right)\right|\tag{7}$$

$$s\left(x\right)=\begin{cases}1, & x>0\\ 0, & x\le 0\end{cases}\tag{8}$$

where g_p ($p=0,\cdots,7$) corresponds to the 8 points of equidistant distribution around the center point, g (i, j) represents the gray value of the center point of the local region.

In the second step, the vertical flip matrices of all the LBP representations above are calculated by right multiplying the sub-unit matrix J_n.

$$\left[LBP_{8,1}^{u2}\left(A_{Lk}\right)\right]^p=LBP_{8,1}^{riu2}\left(A_{Lk}\right)\times J_n,\quad k=1,2,\cdots,M\tag{9}$$

$$\left[LBP_{8,1}^{u2}\left(A_{Rk}\right)\right]^p=LBP_{8,1}^{riu2}\left(A_{Rk}\right)\times J_n,\quad k=1,2,\cdots,M.\tag{10}$$

Then the MMLBP can be generated by averaging the LBP representation of each region with the vertical flip matrix of its symmetric one to alleviate the influence of interference. Therefore, the final representation of the original face image is reestablished by the following formula:

$$LBP_{8,1}^{u2}\left(A_{Lk}\right)=\frac{\left[LBP_{8,1}^{u2}\left(A_{Rk}\right)\right]^p+\left[LBP_{8,1}^{u2}\left(A_{Lk}\right)\right]}{2},\quad k=1,2,\cdots,M\tag{11}$$

$$LBP_{8,1}^{u2}\left(A_{Rk}\right)=\frac{\left[LBP_{8,1}^{u2}\left(A_{Lk}\right)\right]^p+\left[LBP_{8,1}^{u2}\left(A_{Rk}\right)\right]}{2},\quad k=1,2,\cdots,M.\tag{12}$$

Finally, the reconstructed image is normalized to perform the FR tasks. The overall flowchart of the MMLBP method is given in Fig. 3 for better understanding of the procedure. To make comparisons with the original LBP operator described in Section 3.1, some visual results achieved by MMLBP are shown in Fig. 4, here we set M=2. The face images chosen here are the same as those in Fig. 2. The comparison results show that the original LBP operator is not effective at removing interference effects like heterogeneous illumination, occlusion, facial expression and pose variation. In contrast, the MMLBP algorithm can alleviate the influence of interference and thus provide better visual representations of the original faces. More specifically, it removes much of the smooth shading information and hence emphasize local appearance. We can see the obtained representations are much closer to those under well-controlled conditions (frontal expressionless face image under uniform illumination), making it advantageous for FR with only a few images available in the training set.

4 Experiment

In our experiment, the performance of the proposed MMLBP method was evaluated on four famous databases: Yale B, CMU-PIE, AR and FERET, as these four databases contain face images with large illumination, occlusion, facial expression and pose interferences. The images from the same database were cropped to the same

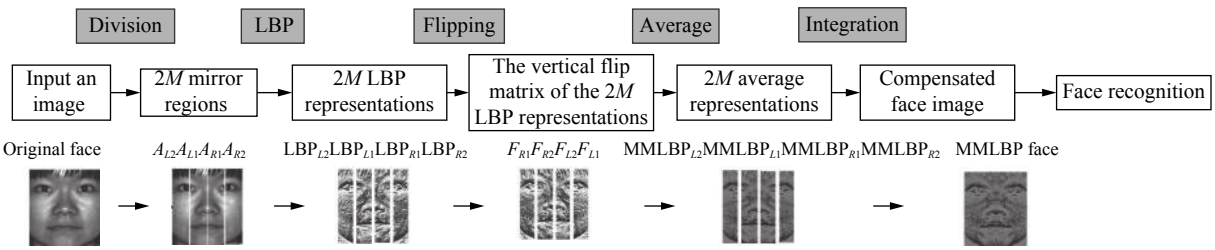

Fig. 3 Overall flowchart of MMLBP and corresponding illustration using M=2

Fig. 4 MMLBP (M=2) used for FR under varying interference

size. And the nearest neighbor classifier based on Euclidean distance was employed for the final recognition and classification. To evaluate the performance of MMLBP algorithm, it was compared to the original LBP operator, the method utilizing the facial symmetry based on original image (SORI), as well as some improved versions of LBP proposed in previous papers: ILBP, MBLBP and LTP. These methods as well as the proposed MMLBP method are all LBP-based operators, but their specific strategies and performances are quite different. ILBP considers both local shape and texture information instead of raw grayscale information and it is only robust to illumination variation[40]. In MBLBP, the computation is done based on average values of block sub regions, instead of individual pixels[41]. Instead of LBP which thresholds at exactly the value of the central pixel, LTP extends to 3-valued codes, in which gray-levels in a zone of width around are quantized to zero, ones above this are quantized to +1 and ones below it to −1[21]. Moreover, face recognition utilizing facial symmetry based on original images SORI and the SSVDR algorithm utilizing the facial symmetry were also employed to make comparisons with the proposed method[42]. Lastly, the method was compared to a state-of-art non-LBP method, called MDML-DCPs, which uses the first derivative of the Gaussian operator to conduct multi-directional filtering to reduce the impact of interferences.

4.1 Experiment on the Yale B database

The Yale B database contains 10 individuals under 64 different illumination conditions and it has been a standard for studies of recognition under variable lighting over the past decade. These images are roughly divided into five subsets according to the direction of the lighting source. Subset 1 contains 70 images of 10 different objects and the lighting source direction is between 0 to 12°. Subsets 2 and 3 both contain 120 images of 10 different objects and the lighting source directions are between 13° and 25°, 26° and 50°, respectively. Subset 4 contains 140 images of 10 different objects and the lighting source direction is between 51° and 77°. Subset 5 contains 190 images of 10 different objects and the lighting source direction is larger than 77°. An example of one object divided into five subsets is shown in Fig. 5.

In order to verify the advantage of the proposed method quantitatively, the images processed by all the methods mentioned above were labelled and classified by the nearest neighbor classifier based on Euclidean distance. Since the performance of the MMLBP method may be influenced by the number of regions, so MMLBP method with M=1, M=2 and M=3 were used in the experiment. Here, we used subset 1 as the training set and all the other subsets were used for testing (shown in Fig. 5). The recognition rates of different methods with the corresponding testing subsets number on the Yale B database were summarized in Table 2, from which we can see that the MMLBP method achieves best recognition accuracy on the whole and defeats all the other approaches when the illumination condition becomes severe. The other methods can also achieve relatively good recognition accuracy when the lighting is tilted slightly, however, when it becomes severe, the recognition rates drop significantly. For example, the recognition rates of LTP are all 100% when testing Subsets 2 and 3. However, when the illumination condition changes, the recognition performance drops dramatically. The worst performance occurs when testing subset 5, the recognition rate is only 56.3%. Similarly, the recognition accuracy of the MBLBP method ranges from 53.6% to 100.0% and that of MDML-DCPs method ranges from 40.5% to 100% with the change of illumination conditions. But the MMLBP methods can still get recognition rates higher than 85% under the worst lighting conditions. The average recognition rates of the MMLBP methods for all M=1, 2 and 3 outperform the other methods.

To further verify our method, we also used subsets 2–5 as the training set respectively, the remaining subsets were used as testing sets, the average recognition rates of all the mentioned methods for the corresponding training subsets were shown in Table 3. According to the results, the MMLBP method shows the best recognition performance regardless of the training subset.

Additionally, the results show that the recognition rate of MMLBP changes with different M values and thus setting a proper M for MMLBP is of great importance. Therefore, we carry out an experiment by testing subset 4 with varying M from 1 to 10. Subsets 1– 3 and 5 are used as training sets, respectively. The recognition rates with varying M are shown in Fig. 6. It can be seen that the recognition rate varies with different training sets, but the overall trend seems to rise first and then

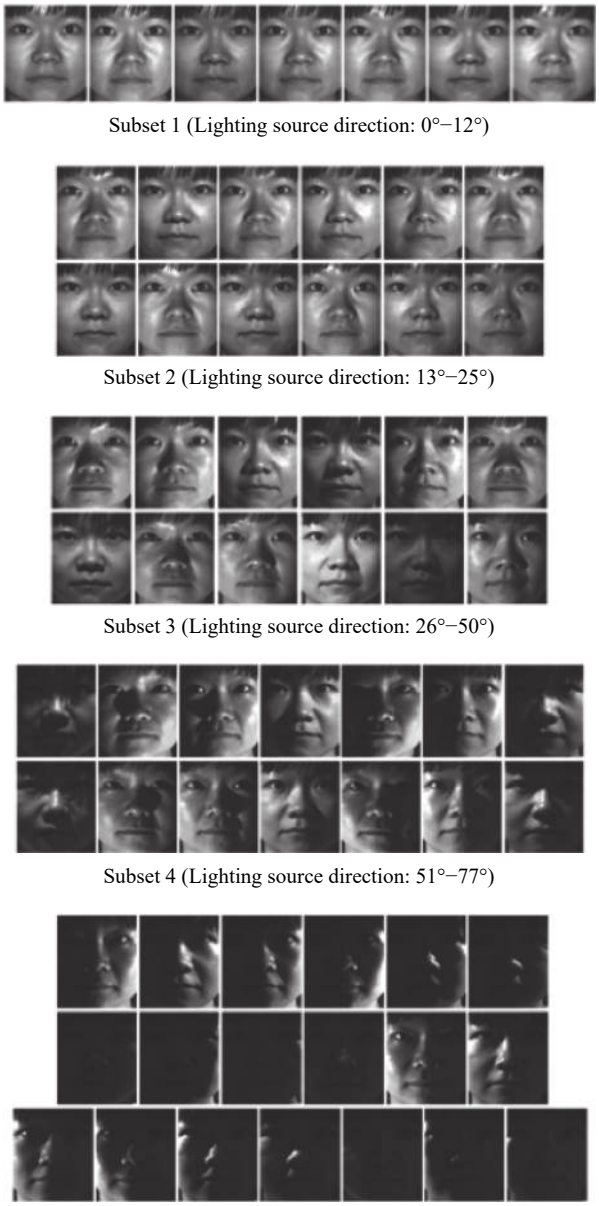

Fig. 5 Sample images of an object from the Yale B divided into five subspaces

drop and rise again with the increase of M. M=3 seems to be a perfect partition structure for carrying out the proposed MMLBP method. The possible reason for this phenomenon might be that the factor M affects the edge of each region, which may happen to be the symmetrical line of the important structure in the face, such as the eyes and nose. Fig.7 shows example images of the mirror partition with M=3. It can be seen that the important structure eyes and nose happen to be divided into two parts which are almost symmetrical.

4.2 Experiment on the CMU PIE database

In the CMU PIE database, there are 68 subjects with varying poses, illumination conditions and expressions (PIE). We chose the images with large illumination variations under five different poses in our experiment. An illustration of the sample images for one person is shown in Fig. 8. All the face images are cropped to the same size.

To begin, we chose some frontally lighted face images of each pose set for training, the rest were used for testing. The specific training and testing set numbers are given in Table 4. All of the methods mentioned above (LBP, ILBP, MBLBP and LTP), together with the proposed MMLBP method with M=1, 2, 3 were applied. The final recognition results were summarized in Table 5. The MMLBP method achieves the best results in all the pose sets, 95.8%, 97.2%, 95.6%, 98.4% and 94.4%, respectively, with M=2 or 3.

In the second experiment, we tested all images as a whole instead of classifying them into groups. Therefore, the FR task was carried out under both illumination and pose interferences. For training the classifier, we used two different sets called training set 1 and training set 2.

Table 2 Recognition rate (%) with training subset 1 under varying lighting conditions on the Yale B database

Methods	Subset 2	Subset 3	Subset 4	Subset 5	Average
ORI	33.3	12.5	11.4	9.0	16.5
LBP	80.8	77.5	42.1	52.1	63.1
ILBP	98.3	99.2	85.7	88.4	92.9
MBLBP	**100.0**	90.8	53.6	71.5	79.0
LTP	**100.0**	**100.0**	68.6	56.3	81.2
SORI	53.3	21.7	12.9	6.8	23.7
SSVDR	75.0	33.3	13.6	7.9	32.5
MDML-DCPs	**100.0**	85.8	70.0	40.5	74.1
MMLBP(M=1)	99.2	99.2	86.4	87.9	93.2
MMLBP(M=2)	99.2	99.2	**87.1**	**88.9**	**93.8**
MMLBP(M=3)	99.2	99.2	**87.1**	88.4	93.5

Table 3 Average recognition rate (%) with different training subsets on the Yale B database

Methods	Subset 1	Subset 2	Subset 3	Subset 4	Subset 5
ORI	16.5	24.1	20.2	12.5	11.2
LBP	63.1	47.0	61.4	35.3	19.6
ILBP	92.9	82.9	80.2	47.0	74.4
MBLBP	79.0	82.3	90.5	56.7	60.3
LTP	81.2	84.7	92.1	37.8	76.3
SORI	23.7	33.4	36.0	12.4	12.25
SSVDR	32.5	36.8	44.1	25.9	35.6
MDML-DCPs	74.1	78.5	76.1	57.2	77.5
MMLBP(M=1)	93.2	92.2	91.5	**64.0**	78.8
MMLBP(M=2)	**93.6**	**93.1**	91.9	58.2	79.2
MMLBP(M=3)	93.5	92.5	**92.4**	58.6	**79.3**

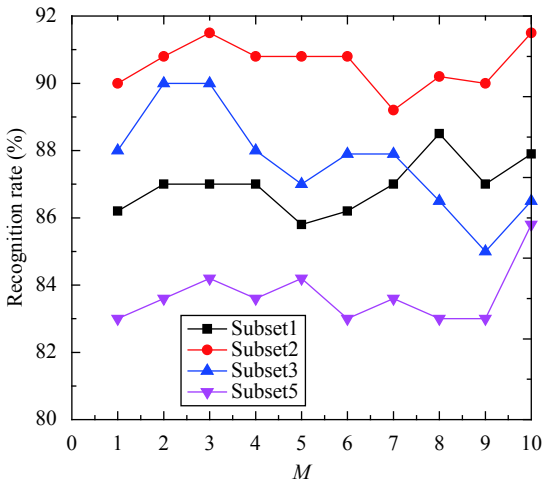

Fig. 6 Recognition rate of MMLBP with varying M

Fig. 7 Example images of mirror partition with M=3

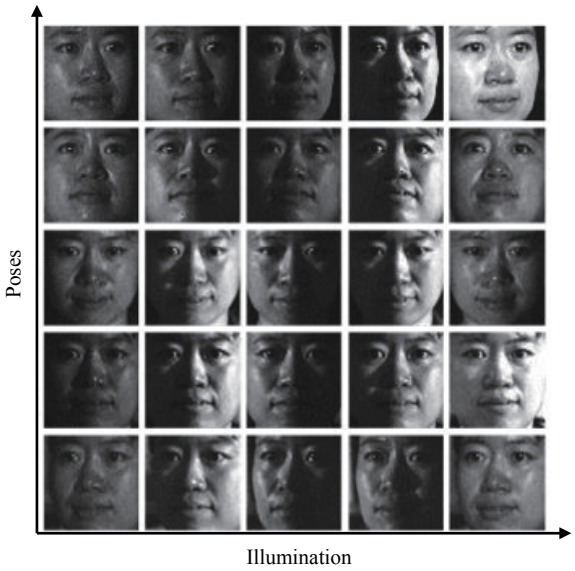

Fig. 8 An illustration of one person in CMU PIE

Table 4 Specific training and testing set number of each pose group on the CMU PIE database

	Pose 1	Pose 2	Pose 3	Pose 4	Pose 5
Training number per subject	5	3	3	5	3
Testing number per subject	38	18	18	38	18

Training set 1 contains images with varying illumination conditions but with the same pose, the same as Pose 2 in Fig. 8. Training set 2, on the contrary, contains frontally lighted face images with the five different poses. The recognition results of all the methods were also given in Table 5 and it can be seen that the MMLBP method still achieves the highest recognition accuracy in testing all the images as a whole no matter what training set is used.

4.3 Experiment on the AR database

The AR database classified into two sessions with varying illumination, expression and occlusions, contains 120 people in total. Each session has 13 images per person numbered from 1 to 13 and 14 to 26, respectively. We used one session for training, and the other for testing. The specific description of the database is tabulated in Table 6. We also displayed the sample images of an individual in one session of the AR database in Fig. 9.

To evaluate the performance of the proposed MMLBP method, several experiments were conducted on different subsets in AR database, and the results obtained were tabulated in Table 7. According to the results, the MMLBP method defeats all the other approaches in all the subsets, i.e., the proposed method shows great robustness in illumination, occlusion and expression interferences.

4.4 Experiment on the FERET database

The FERET is a result of the FERET program, which was sponsored by the US Department of Defense through the DARPA program. It contains 1 400 images of 200 individuals with seven different images of each individual varying in illumination, expression and pose. In our experiments, all face images were aligned, cropped and resized to 80 × 80 pixel based on the location of the eyes. The sample images of an individual in FERET database are shown in Fig. 10.

In our experiment, we used the full-faced and strictly centered images for training, which were the same as the first images in Fig. 10. The remaining images varying in pose, expression and illumination are used for testing. The final recognition results are shown in Table 8. As seen from the results, the MMLBP method again obtains better recognition results compared with the other state-of-the-art approaches.

5 Conclusions

In this study, a novel and robust descriptor MMLBP was proposed to deal with the image interference problem in FR. To alleviate the impact of various interferences and improve FR performance, the proposed method here combines LBP with multi-mirror facial symmetry (MMLBP) by dividing the face image into multi-mirror regions. MMLBP offers the following advantages: 1) It is capable of adaptively compensating lighting under heterogeneous lighting conditions; 2) It generates ex-

Table 5 Recognition rate (%) of different subset on the CMU PIE database

Methods	ORI	LBP	ILBP	MBLBP	LTP	SORI	SSVDR	MDML-DCPs	MMLBP(M=1)	MMLBP(M=2)	MMLBP(M=3)
Pose 1	19.7	92.6	86.6	85.5	92.1	20.5	42.9	91.3	92.6	**95.8**	92.9
Pose 2	26.1	91.7	86.7	85.0	78.3	27.2	46.1	95.5	95.0	96.1	**97.2**
Pose 3	24.4	93.3	75.0	85.6	91.7	27.7	36.7	93.9	93.3	94.4	**95.6**
Pose 4	19.5	84.2	94.0	77.4	94.5	20.7	38.9	96.3	96.3	**98.4**	96.3
Pose 5	24.4	88.3	66.7	87.8	84.4	25.0	36.7	91.1	85.6	93.3	**94.4**
Training set 1	47.8	66.4	63.0	60.6	75.0	49.9	43.5	76.4	70.8	**76.9**	76.1
Training set 2	12.5	67.8	51.9	76.6	75.5	13.8	22.2	85.1	83.0	84.2	**86.2**

Table 6 Distribution of AR database in different sets

	Session 1 images (Training set)	Session 2 images (Test set)
Change in expressions	1, 5–7	14, 18–20
Varying illumination	1–4	14–17
Sunglass with illumination changes	8–10	21–23
Scarf with illumination changes	11–13	24–26

Fig. 9 Sample images of an individual in one session in the AR database

Table 7 Recognition rate (%) of different subset on the AR database

Image variations	ORI	LBP	ILBP	MBLBP	LTP	SORI	SSVDR	MDML-DCPs	MMLBP(M=1)	MMLBP(M=2)	MMLBP(M=3)
Change in expressions	27.5	60.0	92.5	92.5	92.5	27.5	77.5	87.5	90.0	92.5	**95.0**
Varying illumination	45.0	90.0	90.0	92.5	95.0	60.0	60.0	95.0	92.5	**97.5**	92.5
Sunglass with illumination changes	30.0	73.3	80.0	90.0	93.3	56.7	50.0	86.7	**93.3**	83.3	83.3
Scarf with illumination changes	46.7	56.7	70.0	70.0	76.7	50.0	36.7	46.7	66.7	**76.7**	73.7
Total images	37.2	70.7	84.3	87.1	90.0	48.6	56.1	68.5	86.4	**88.6**	87.2

Fig. 10 Sample images of one session in the AR database

tracted image features that are much closer to those under well-controlled conditions (i.e., frontal facial images without expression), and therefore successfully handles various image interferences that are common in FR applications without preprocessing operation and a large number of training images. The proposed method was validated with four public data sets (i.e., Yale B, CMU PIE, AR and FERET). In contrast with the original LBP, the method utilizing the facial symmetry based on original image (SORI), its later variations (ILBP, MBLBP and LTP), the SSVDR algorithm utilizing the facial symmetry and a state-of-art non-LBP method MDML-DCPs, it is shown with greater FR robustness and performance for images with interferences including illumination, occlusion, facial expression and pose variations. The MMLBP method, however, has minor drawbacks. Since the method relies on the symmetry of human faces, it will likely be less effective for face images that reveal facial defects. For future research, we would like to explore the influence of varying face ages and image resolution using the MMLBP method, while further improving recognition performance.

Acknowledgements

The work was supported by National Natural Science Foundation of China (No. 51305392), Youth Funds of the State Key Laboratory of Fluid Power Transmission and Control (No. SKLoFP_QN_1501), Zhejiang Provincial

Table 8 Recognition rate (%) on the FERET database

Methods	ORI	LBP	ILBP	MBLBP	LTP	SORI	SSVDR	MDML-DCPs	MMLBP(M=1)	MMLBP(M=2)	MMLBP(M=3)
Recognition rates	15.0	40.0	46.7	48.3	31.7	25.0	20.0	55.0	56.7	55.0	**58.3**

Natural Science Foundation of China (Nos. LY17E050009 and LZ15E050001), and the Fundamental Rsesearch Funds for the Central Universities (No. 2018QNA4008).

References

[1] J. V. Haxby, M. I. Gobbini, M. L. Furey, A. Ishai, J. L. Schouten, P. Pietrini. Distributed and overlapping representations of faces and objects in ventral temporal cortex. *Science*, vol. 293, no. 5539, pp. 2425–2430, 2001. DOI: 10.1126/science.1063736.

[2] X. F. He, S. C. Yan, Y. X. Hu, P. Niyogi, H. J. Zhang. Face recognition using Laplacianfaces. *IEEE Transactions on Pattern Analysis and Machine Intelligence*, vol. 27, no. 3, pp. 328–340, 2005. DOI: 10.1109/TPAMI.2005.55.

[3] J. Wright, A. Y. Yang, A. Ganesh, S. S. Sastry, Y. Ma. Robust face recognition via sparse representation. *IEEE Transactions on Pattern Analysis and Machine Intelligence*, vol. 31, no. 2, pp. 210–227, 2009. DOI: 10.1109/TPAMI.2008.79.

[4] I. Naseem, R. Togneri, M. Bennamoun. Linear regression for face recognition. *IEEE Transactions on Pattern Analysis and Machine Intelligence*, vol. 32, no. 11, pp. 2106–2112, 2010. DOI: 10.1109/TPAMI.2010.128.

[5] L. S. Qiao, S. C. Chen, X. Y. Tan. Sparsity preserving projections with applications to face recognition. *Pattern Recognition*, vol. 43, no. 1, pp. 331–341, 2010. DOI: 10.1016/j.patcog.2009.05.005.

[6] H. S. Du, Q. P. Hu, D. F. Qiao, I. Pitas. Robust face recognition via low-rank sparse representation-based classification. *International Journal of Automation and Computing*, vol. 12, no. 6, pp. 579–587, 2015. DOI: 10.1007/s11633-015-0901-2.

[7] X. Geng, Z. H. Zhou, K. Smith-Miles. Automatic age estimation based on facial aging patterns. *IEEE Transactions on Pattern Analysis and Machine Intelligence*, vol. 29, no. 12, pp. 2234–2240, 2007. DOI: 10.1109/TPAMI.2007.70733.

[8] U. Park, Y. Y. Tong, A. K. Jain. Age-invariant face recognition. *IEEE Transactions on Pattern Analysis and Machine Intelligence*, vol. 32, no. 5, pp. 947–954, 2010. DOI: 10.1109/TPAMI.2010.14.

[9] X. Geng, C. Yin, Z. H. Zhou. Facial age estimation by learning from label distributions. *IEEE Transactions on Pattern Analysis and Machine Intelligence*, vol. 35, no. 10, pp. 2401–2412, 2013. DOI: 10.1109/TPAMI.2013.51.

[10] K. Jia, S. G. Gong. Hallucinating multiple occluded face images of different resolutions. *Pattern Recognition Letters*, vol. 27, no. 15, pp. 1768–1775, 2006. DOI: 10.1016/j.patrec.2006.02.009.

[11] C. X. Ren, D. Q. Dai, H. Yan. Coupled kernel embedding for low-resolution face image recognition. *IEEE Transactions on Image Processing*, vol. 21, no. 8, pp. 3770–3783, 2012. DOI: 10.1109/TIP.2012.2192285.

[12] W. W. W. Zou, P. C. Yuen. Very low resolution face recognition problem. *IEEE Transactions on Image Processing*, vol. 21, no. 1, pp. 327–340, 2012. DOI: 10.1109/TIP.2011.2162423.

[13] N. Alyuz, B. Gokberk, L. Akarun. Regional registration for expression resistant 3D face recognition. *IEEE Transactions on Information Forensics and Security*, vol. 5, no. 3, pp. 425–440, 2010. DOI: 10.1109/TIFS.2010.2054081.

[14] H. Drira, B. Ben Amor, A. Srivastava, M. Daoudi, R. Slama. 3D face recognition under expressions, occlusions, and pose variations. *IEEE Transactions on Pattern Analysis and Machine Intelligence*, vol. 35, no. 9, pp. 2270–2283, 2013. DOI: 10.1109/TPAMI.2013.48.

[15] F. K. Zaman, A. A. Shafie, Y. M. Mustafah. Robust face recognition against expressions and partial occlusions. *International Journal of Automation and Computing*, vol. 13, no. 4, pp. 319–337, 2016. DOI: 10.1007/s11633-016-0974-6.

[16] X. Z. Zhang, Y. S. Gao. Face recognition across pose: A review. *Pattern Recognition*, vol. 42, no. 11, pp. 2876–2896, 2009. DOI: 10.1016/j.patcog.2009.04.017.

[17] G. Passalis, P. Perakis, T. Theoharis, I. A. Kakadiaris. Using facial symmetry to handle pose variations in real-world 3D face recognition. *IEEE Transactions on Pattern Analysis and Machine Intelligence*, vol. 33, no. 10, pp. 1938–1951, 2011. DOI: 10.1109/TPAMI.2011.49.

[18] H. C. Zhang, Y. N. Zhang, T. S. Huang. Pose-robust face recognition via sparse representation. *Pattern Recognition*, vol. 46, no. 5, pp. 1511–1521, 2013. DOI: 10.1016/j.patcog.2012.10.025.

[19] K. C. Lee, J. Ho, D. J. Kriegman. Acquiring linear subspaces for face recognition under variable lighting. *IEEE Transactions on Pattern Analysis and Machine Intelligence*, vol. 27, no. 5, pp. 684–698, 2005. DOI: 10.1109/TPAMI.2005.92.

[20] W. C. Kao, M. C. Hsu, Y. Y. Yang. Local contrast enhancement and adaptive feature extraction for illumination-invariant face recognition. *Pattern Recognition*, vol. 43, no. 5, pp. 1736–1747, 2010. DOI: 10.1016/j.patcog.2009.11.016.

[21] X. Y. Tan, B. Triggs. Enhanced local texture feature sets for face recognition under difficult lighting conditions. *IEEE Transactions on Image Processing*, vol. 19, no. 6, pp. 1635–1650, 2010. DOI: 10.1109/TIP.2010.2042645.

[22] V. Struc, J. Zibert, N. Pavesic. Histogram remapping as a preprocessing step for robust face recognition. *WSEAS Transactions on Information Science and Applications*, vol. 6, no. 3, pp. 520–529, 2009.

[23] P. H. Lee, S. W. Wu, Y. P. Hung. Illumination compensation using oriented local histogram equalization and its application to face recognition. *IEEE Transactions on Image Processing*, vol. 21, no. 9, pp. 4280–4289, 2012. DOI: 10.1109/TIP.2012.2202670.

[24] Y. Cheng, Y. K. Hou, C. X. Zhao, Z. Y. Li, Y. Hu, C. L. Wang. Robust face recognition based on illumination invariant in nonsubsampled contourlet transform domain. *Neurocomputing*, vol. 73, no. 10–12, pp. 2217–2224, 2010. DOI: 10.1016/j.neucom.2010.01.012.

[25] Y. Adini, Y. Moses, S. Ullman. Face recognition: The problem of compensating for changes in illumination direction. *IEEE Transactions on Pattern Analysis and Machine Intelligence*, vol. 19, no. 7, pp. 721–732, 1997. DOI: 10.1109/34.598229.

[26] A. S. Georghiades, P. N. Belhumeur, and D. J. Kriegman. From few to many: Illumination cone models for face recognition under variable lighting and pose. *IEEE Transactions on Pattern Analysis and Machine Intelligence*, vol. 23, no. 6, pp. 643–660, 2001. DOI: 10.1109/34.927464.

[27] J. Y. Zhu, W. S. Zheng, F. Lu, J. H. Lai. Illumination invariant single face image recognition under heterogeneous lighting condition. *Pattern Recognition*, vol. 66, pp. 313–

327, 2017. DOI: 10.1016/j.patcog.2016.12.029.

[28] A. Shashua, T. Riklin-Raviv. The quotient image: Class-based re-rendering and recognition with varying illuminations. *IEEE Transactions on Pattern Analysis and Machine Intelligence*, vol. 23, no. 2, pp. 129–139, 2001. DOI: 10.1109/34.908964.

[29] H. T. Wang, S. Z. Li, Y. S. Wang. Face recognition under varying lighting conditions using self quotient image. In *Proceedings of the 6th IEEE International Conference on Automatic Face and Gesture Recognition*, IEEE, Seoul, South Korea, pp. 819–824, 2004. DOI: 10.1109/AFGR.2004.1301635.

[30] T. P. Zhang, Y. Y. Tang, B. Fang, Z. W. Shang, X. Y. Liu. Face recognition under varying illumination using gradientfaces. *IEEE Transactions on Image Processing*, vol. 18, no. 11, pp. 2599–2606, 2009. DOI: 10.1109/TIP.2009.2028255.

[31] J. Kim, J. Choi, J. Yi, M. Turk. Effective representation using ICA for face recognition robust to local distortion and partial occlusion. *IEEE Transactions on Pattern Analysis and Machine Intelligence*, vol. 27, no. 12, pp. 1977–1981, 2005. DOI: 10.1109/TPAMI.2005.242.

[32] K. Wang, X. X. Long, R. F. Li, L. J. Zhao. A discriminative algorithm for indoor place recognition based on clustering of features and images. *International Journal of Automation and Computing*, vol. 14, no. 4, pp. 407–419, 2017. DOI: 10.1007/s11633-017-1081-z.

[33] Y. Tai, J. Yang, Y. G. Zhang, L. Luo, J. J. Qian, Y. Chen. Face recognition with pose variations and misalignment via orthogonal Procrustes regression. *IEEE Transactions on Image Processing*, vol. 25, no. 6, pp. 2673–2683, 2016. DOI: 10.1109/TIP.2016.2551362.

[34] B. Zhao, J. S. Feng, X. Wu, S. C. Yan. A survey on deep learning-based fine-grained object classification and semantic segmentation. *International Journal of Automation and Computing*, vol. 14, no. 2, pp. 119–135, 2017. DOI: 10.1007/s11633-017-1053-3.

[35] U. Prabhu, J. Heo, M. Savvides. Unconstrained pose-invariant face recognition using 3D generic elastic models. *IEEE Transactions on Pattern Analysis and Machine Intelligence*, vol. 33, no. 10, pp. 1952–1961, 2011. DOI: 10.1109/TPAMI.2011.123.

[36] M. Merras, S. El Hazzat, A. Saaidi, K. Satori, A. G. Nazih. 3D face reconstruction using images from cameras with varying parameters. *International Journal of Automation and Computing*, vol. 14, no. 6, pp. 661–671, 2017. DOI: 10.1007/s11633-016-0999-x.

[37] T. Ojala, M. Pietikäinen, D. Harwood. A comparative study of texture measures with classification based on feature distributions. *Pattern Recognition*, vol. 29, no. 1, pp. 51–59, 1996. DOI: 10.1016/0031-3203(95)00067-4.

[38] T. Ahonen, A. Hadid, M. Pietikäinen. Face description with local binary patterns: Application to face recognition. *IEEE Transactions on Pattern Analysis & Machine Intelligence*, vol. 28, no. 12, pp. 2037–2041, 2006. DOI: 10.1109/TPAMI.2006.244.

[39] T. Ahonen, A. Hadid, M. Pietikäinen. Face recognition with local binary patterns. In *Proceedings of European Conference on Computer Vision*, Prague, Czech Republic, pp. 469–481, 2004. DOI: 10.1007/978-3-540-24670-1_36.

[40] H. L. Jin, Q. S. Liu, H. Q. Lu, X. F. Tong. Face detection using improved LBP under bayesian framework. In *Proceedings of the 3rd International Conference on Image and Graphics*, IEEE, Hong Kong, China, pp. 306–309, 2004. DOI: 10.1109/ICIG.2004.62.

[41] S. C. Liao, X. X. Zhu, Z. Lei, L. Zhang, S. Z. Li. Learning multi-scale block local binary patterns for face recognition. In *Proceedings of International Conference on Biometrcs*, Seoul, Korea, pp. 828–837, 2007. DOI: 10.1007/978-3-540-74549-5_87.

[42] Y. H. Chen, S. G. Tong, F. Y. Cong, J. Xu. Symmetrical singular value decomposition representation for pattern recognition. *Neurocomputing*, vol. 214, pp. 143–154, 2016. DOI: 10.1016/j.neucom.2016.05.075.

[43] C. X. Ding, J. Choi, D. C. Tao, L. S. Davis. Multi-directional multi-level dual-cross patterns for robust face recognition. *IEEE Transactions on Pattern Analysis and Machine Intelligence*, vol. 38, no. 3, pp. 518–531, 2016. DOI: 10.1109/TPAMI.2015.2462338.

[44] P. J. Phillips, H. Moon, S. A. Rizvi, P. J. Rauss. The FERET evaluation methodology for face-recognition algorithms. *IEEE Transactions on Pattern Analysis and Machine Intelligence*, vol. 22, no. 10, pp. 1090–1104, 2000. DOI: 10.1109/34.879790.

[45] B. Yang, S. C. Chen. A comparative study on local binary pattern (LBP) based face recognition: LBP histogram versus LBP image. *Neurocomputing*, vol. 120, pp. 365–379, 2013. DOI: 10.1016/j.neucom.2012.10.032.

[46] Z. Wang, A. C. Bovik, H. R. Sheikh, E. P. Simoncelli. Image quality assessment: From error visibility to structural similarity. *IEEE Transactions on Image Processing*, vol. 13, no. 4, pp. 600–612, 2004. DOI: 10.1109/TIP.2003.819861.

Shui-Guang Tong received the M. Sc. degree in mechanical engineering from Nanjing University of Science and Technology, China in 1987, and the Ph. D. degree in mechanical engineering from Zhejiang University, China in 1991. Since 1996, he has been a professor at Zhejiang University, China. He has published about 100 refereed journal and conference papers. He is the professor of Mechanical Engineering, Zhejiang University, deputy dean of the Industrial Technology Research Institute, Zhejiang University, director of the Institute of Mechanical Design, Zhejiang University, China.

His research interests include fault diagnosis, structure optimization, and pattern recognition.

E-mail: cetongsg@zju.edu.cn

ORCID iD: 0000-0002-4837-6432

Yuan-Yuan Huang received the B. Sc. degree in mechanical engineering and automation from North China Electric Power University, China in 2016. Now, she is a Ph. D. degree candidate in State Key Laboratory of Fluid Power and Mechatronic Systems, Zhejiang University, China.

Her research interests include pattern recognition, fault diagnosis and signal processing.

E-mail: huang_yy@zju.edu.cn

Zhe-Ming Tong received the B.Sc. degree in mechanical engineering from University of Wisconsin-Madison, USA in 2010, the MSc. and Ph.D. degrees in mechanical engineering from Cornell University, USA in 2015. Prior to joining Zhejiang University, he was a research associate at the Center for Green Buildings and Cities, Harvard University, USA. He is a research professor (tenure-track) at School of Mechanical Engineering, Zhejiang University, China. He was selected to "The 1000-talents Plan for Distinguished Young Scholars" by the Government of China, and "The Bairen Distinguished Young Faculty Program" by Zhejiang University, China in 2017. Dr. Tong's research group primarily focuses on advanced characterization of vehicle emission, sustainable built environments, and cabin environmental quality of motor vehicles. In the past five years, he has authored more than 20 technical papers, most of which were published in top international journals, such as *Environmental Science Technology*, *Environment International*, and *Applied Energy*. Several of his articles were selected as ESI hot and highly cited papers that received a much higher than average number of citations. He is a member of American Association for Aerosol Research (AAAR), American Society of Heating, Refrigerating and Air Conditioning Engineer (ASHRAE), and American Chemical Society (ACS). He also regularly serves as a peer reviewer for more than 20 international journals. He also holds a number of patents through industrial collaborations.

His research interests include man-machine engineering, energy optimization management of new energy vehicles and multiphase flow numerical simulation technology.

E-mail: tzm@zju.edu.cn (Corresponding author)
ORCID iD: 0000-0002-0436-2370